ChemComm

COMMUNICATION

View Article Online
View Journal

Cite this: DOI: 10.1039/d0cc06518h

Received 11th November 2020,
Accepted 30th November 2020

DOI: 10.1039/d0cc06518h

rsc.li/chemcomm

Low-spin 1,1′-diphosphametallocenates of chromium and iron†

Samuel M. Greer, [abc] Ökten Üngor, [b] Ross J. Beattie, [a] Jaqueline L. Kiplinger, *[a] Brian L. Scott, [a] Benjamin W. Stein *[a] and Conrad A. P. Goodwin *[ad]

We report two anionic diphosphametallocenates, [K(2.2.2-crypt)][M(PC$_4$Me$_4$)$_2$] (M = Cr, 2-Cr; Fe, 2-Fe). Both are low-spin ($S = \frac{1}{2}$) by EPR spectroscopy and SQUID magnetometry. This contrasts the high-spin ($S = \frac{3}{2}$) ferrocenate, [K(2.2.2-crypt)][Fe(C$_5$H$_2$-1,2,4-^{t}Bu)$_2$] (4-Fe). Quantum chemical calculations suggest this is due to significant differences in ligand field splitting of the d-orbitals which also explain structural features in the 2-M complexes.

The chemistry and electronic structure of transition metal (TM) metallocenes[1,2] has fascinated chemists since the discovery of ferrocene, [Fe(Cp)$_2$] (FcH, Cp = cyclopentadienyl, {C$_5$H$_5$}).[3] Oxidation of FcH leads to the ferrocenium cation, [Fe(Cp)$_2$]$^+$ (FcH$^+$),[4] which finds use in organic synthesis,[5] while the FcH$^{+/0}$ couple serves as an electrochemical standard.[6] "Heterometallocenes" are related complexes that feature heterocycles in lieu of Cp ligands (*e.g.* η^5-pyrrolides, {NC$_4$R$_4$}$^-$; η^5-stannolides {SbC$_4$R$_4$}$^-$; poly-phospholides {P$_n$C$_{5-n}$R$_{5-n}$}$^-$ *etc.*).[7] The exchange of C atoms for heteroatoms can lead to drastic changes in reactivity.[1,2] For example, ferrocene undergoes deprotonation by alkyl-lithium reagents,[8,9] but 1,1′-diphosphaferrocenes undergo nucleophilic attack at the P atom.[10,11]

The oxidation of TM metallocenes to metallocenium cations is a defining feature of their chemistry, with examples across the first row transition metals (V–Ni).[1,12] The corresponding reductive chemistry is underdeveloped outside of electrochemical studies.[13] Exceptions include the synthesis of [Mn(Cp*)$_2$]$^-$ salts,[14] the reduction of [Co{η^5-C$_9$H$_5$-1,3-(SiMe$_3$)$_2$}$_2$] to a formally anionic "cobaltate",[15] and an anionic iron bis-stannolide.[7c] Some of us have recently described the chemical reduction of [M(Cp^{ttt})$_2$] (**3-M**; M = Mn, Fe, Co; Cp^{ttt} = {C$_5$H$_2$-1,2,4-^{t}Bu}) to [K(2.2.2-crypt)][M(Cp^{ttt})$_2$] (**4-M**; M = Mn, Fe, Co) giving an 18, 19 and 20 valence electron (VE) series,[16] similar to the 17, 18, 19 VE series of [Fe(Cp^R)(arene)]$^{2+/+/0}$ complexes.[17]

The synthesis of 3d metallocene anions could open up the possibility of using them as nucleophiles like "A[Re(Cp)$_2$]" (A = Li,[18] K[19]). While the [Mn(Cp*)$_2$]$^-$ anion is temperature stable,[14c,a] analogous [FcH]$^-$ and [Fe(Cp*)$_2$]$^-$ anions are not easily accessed chemically;[13b] and **4-M** complexes are extremely temperature sensitive.[16] We sought ligands that would impart greater stability to the anionic species. Reports of [M(PC$_4$R$_n$H$_{4-n}$)$_2$] for a range of metals include the Fe/Ru/Os triad,[7d,20] and many exhibit facile redox chemistry.[21] For example, [M(TMP)$_2$] (M = Cr, **1-Cr**;[22] Fe, **1-Fe**;[23] TMP = {PC$_4$Me$_4$}) have M$^{+/0}$ couples (*vs.* FcH$^{+/0}$: M = Cr, −0.77 V;[24] Fe, 0.06 V), and M$^{0/-}$ (*vs.* FcH$^{+/0}$: M = Cr, −2.4 V; Fe, −3.02 V) at less cathodic potentials than **3-M**.[16] Here we report the synthesis of 1,1′-diphosphametallocenates, [K(2.2.2-crypt)][M(TMP)$_2$] (M = Cr, **2-Cr**; Fe, **2-Fe**), by low-temperature reduction of **1-M** by KC$_8$ in the presence of 2.2.2-cryptand (Scheme 1).

Precursor **1-M** (M = Cr, Fe) were synthesized from MCl$_2$ and base-free KTMP by modification of literature procedures.[21b,23b] During the course of this work we have also structurally characterized [Zr(Cp)$_2$(C$_4$Me$_4$)] (**5**) and Ph-TMP (**6**) for the first time, which are precursors in the synthesis of KTMP (see ESI†). Complexes **1-M** were then reduced under conditions

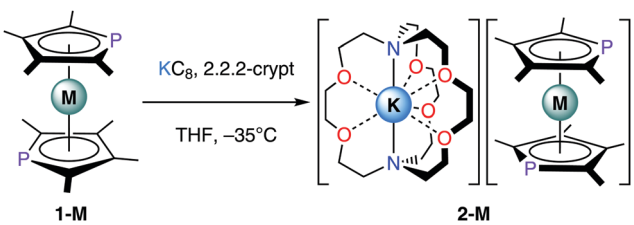

1-M 2-M

Scheme 1 Synthesis of **2-M** (M = Cr, Fe) from **1-M**, KC$_8$ and 2.2.2-cryptand.

[a] *Chemistry Division, Los Alamos National Laboratory, Los Alamos, NM 87545, USA. E-mail: kiplinger@lanl.gov, bstein@lanl.gov, cgoodwin@lanl.gov*
[b] *National High Magnetic Field Laboratory, Florida State University, Tallahassee, FL 32310, USA*
[c] *Department of Chemistry & Biochemistry, Florida State University, Tallahassee, FL 32306, USA*
[d] *Department of Chemistry, School of Natural Sciences, The University of Manchester, Oxford Road, Manchester, M13 9PL, UK*

† Electronic supplementary information (ESI) available. CCDC 2003385–2003390, 2017380 and 2017381. For ESI and crystallographic data in CIF or other electronic format see DOI: 10.1039/d0cc06518h

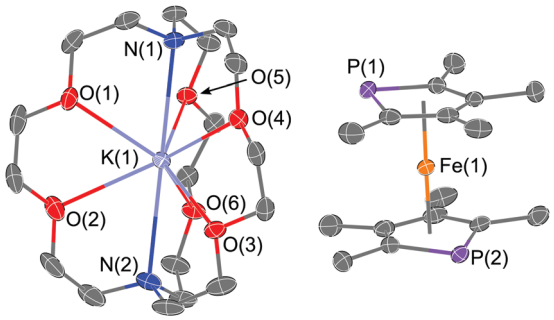

Fig. 1 Molecular structure of **2-Fe** with selective atom labelling (C = grey, P = purple, K = violet, Fe = orange, N = blue, O = red). Displacement ellipsoids set at 50% probability level and H-atoms omitted for clarity.

established for the synthesis of low-valent metallocenes.[16,25] Addition of solid KC_8 to cooled (−35 °C) solutions of **1-M** and 2.2.2-crypt in THF caused rapid color changes (from red to red-brown, **2-Cr**; or red to green-black, **2-Fe**). Intensely colored crystals of **2-Cr** and **2-Fe** were obtained upon workup (Fig. 1 and ESI†).

These specific Cr and Fe complexes (**1-Cr** and **1-Fe**) were chosen as they have established redox chemistry and thus provided an ideal testbed for the comparison of spin-states in reduced metallocenes.[22,23] We were unable to synthesize **1-Mn** and **1-Co** in order to furnish a redox series from Cr^{2+} (d^4) to Co^{1+} (d^8). Reactions between Mn^{2+} halides and KTMP gave intractable mixtures. For Co^{2+} we could isolate traces of impure $[Co(\eta^5\text{-TMP})(\mu{:}\eta^1{:}\eta^1\text{-TMP})]_2$ (7) (ESI†).

Salient structural parameters for **1-M** are shown along with those of **2-M** in Table 1. Complexes **2-M** (M = Cr, Fe) are isomorphous, their ATR-FTIR spectra are superimposable, and elemental analysis results were in excellent agreement with prediction. The structures contain discrete [K(2.2.2-crypt)] cations, and $[M(TMP)_2]$ anions. In **2-M** the TMP-P atoms are each situated opposite a β-carbon of the second ring, similar to neutral $[Fe(PC_4H_2\text{-}2,5\text{-}Me_2)_2]$.[26] Upon reduction there is a small decrease in M–P distances for Cr (Δ = −0.022(1) Å) but an increase for Fe (Δ = +0.103(1) Å); and changes in the $TMP_{cent}\cdots M$ distances follow the same trend (Cr, Δ = −0.057 Å; Fe, Δ = +0.053 Å). The $TMP_{cent}\cdots Cr$ change between d^4 **1-Cr** (1.795(1) Å) and d^5 **2-Cr** (avg. 1.738(1) Å) is similar to the $Cp^*_{cent}\cdots Mn$ change between d^4 and d^5 manganocenes.[27] The $TMP_{cent}\cdots Fe$ change between d^6 **1-Fe** (1.660(1) Å) and d^7 **2-Fe** (avg. 1.713(1) Å) is larger than the increase from **3-Fe** (avg. 1.715(2) Å) to **4-Fe** (avg. 1.750(3) Å), likely as the distances in **3-Fe** are due to the bulky ligands rather than electronic effects.[16]

Table 1 Selected structural parameters for **1-M** and **2-M**

	1-Cr	2-Cr	1-Fe	2-Fe
P–M/Å	2.3812(4)	2.3596(8) 2.3595(7)	2.2932(4)	2.3842(8) 2.4078(7)
$TMP_{cent}\cdots M$/Å	1.795(1)	1.739(1) 1.737(1)	1.660(1)	1.714(1) 1.711(1)
$PC_{2plane}\cdots C_{4plane}$/°	4.45(12)	3.57(2) 4.64(2)	1.27(13)	6.58(2) 8.73(2)
TMP-P_2 twist angle/°	180	139.82(5)	180	146.35(5)

The ^1H, $^{13}C\{^1H\}$, and $^{31}P\{^1H\}$ NMR spectra of **2-M** were largely uninformative (ESI†) due to paramagnetic broadening and diamagnetic impurities which dominate the spectra. However, in the ^1H NMR spectrum of **2-Fe** we observed three broad peaks ($\nu_{1/2}$ < 17 Hz) in the range 3.37–3.30 ppm corresponding to 2.2.2-crypt; a doublet at 2.19 ppm ($^3J_{HP}$ = 10.29 Hz) and a singlet at 1.94 ppm correspond to TMP ligand resonances. Complex **2-Cr** could be heated in THF solution (up to 50 °C) and recrystallized with >80% recovery of material, whereas THF solutions of **2-Fe** show decomposition in the ^1H NMR spectrum over the course of an hour at room temperature. Data for **1-M** have been reported previously.

We have employed SQUID magnetometry to measure the susceptibility of the open-shell complexes. **1-Cr** and **2-Cr** exhibit χT (298 K) values of ∼1.24 and ∼0.38 emu K mol^{-1} (Fig. S34, ESI†) which suggest S = 1 as previously reported,[21b] and $S = \frac{1}{2}$ respectively. The observed χT (298 K) value of **2-Fe** (∼0.26 emu K mol^{-1}) is less than the spin-only value for an $S = \frac{1}{2}$ system (0.375 emu K mol^{-1}) (Fig. 2 and Fig. S35, ESI†), which we attribute to some thermal decomposition of paramagnetic **2-Fe** to diamagnetic **1-Fe**, as well as weighing errors and diamagnetic corrections affecting this weakly paramagnetic system. As magnetic measurements were inconclusive for **2-Fe**, we turned to high-field electron paramagnetic resonance (EPR) spectroscopy to determine the ground state spin of **2-Cr** and **2-Fe**. These measurements reveal spectra that are typical of complexes where $S = \frac{1}{2}$. The spectrum of **2-Cr** is nearly axial with g_1 = 2.023(5), g_2 = 1.993(5), and g_3 = 1.985(5) (Fig. S32, ESI†); and **2-Fe** exhibits a rhombic signal (Fig. 2b) with g_1 = 2.033(5), g_2 = 1.999(5), and g_3 = 1.943(5), which is similar to other low-spin Fe^{1+} sandwich complexes.[17]

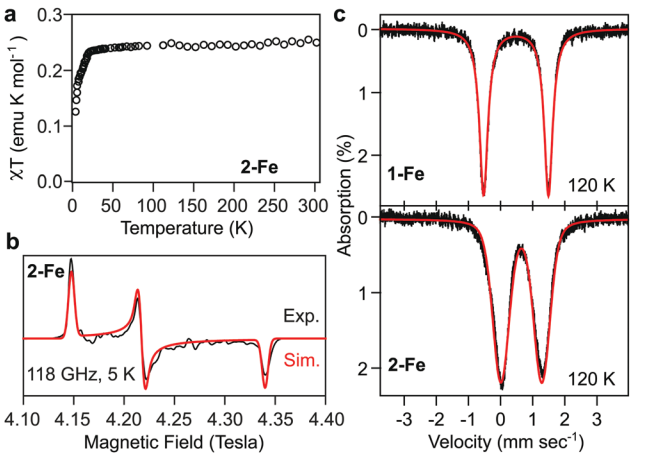

Fig. 2 (a) Temperature dependence of χT for **2-Fe**; (b) experimental (black) and simulated (red) EPR spectra of **2-Fe** recorded at 118 GHz and 5 K. The spectrum is simulated with g_1 = 2.033, g_2 = 1.999, and g_3 = 1.943. Baseline features in the **2-Fe** spectrum result from polycrystallinity. A minor signal arising from an unidentified impurity at lower field is omitted (see Fig. S28, ESI†); (c) experimental (black) and simulated (red) ^{57}Fe Mössbauer spectra of **1-Fe** and **2-Fe**. Simulations were generated for **1-Fe** using δ = 0.48(3), ΔE_Q = 2.02(2) mm s^{-1}, and for **2-Fe** with δ = 0.65(4), ΔE_Q = 1.28(4) mm s^{-1}.

^{57}Fe Mössbauer spectroscopy was used to further investigate the differences between **1-Fe** and **2-Fe** which display a single quadrupole doublet in each spectrum (at 120 K, Fig. 2c). The parameters for **1-Fe**, **2-Fe**, **3-Fe** and **4-Fe** are summarized in Table 2. The more positive isomer shift (δ) of **2-Fe** suggests that there is decreased s-orbital electron density at the Fe nucleus compared to that in **1-Fe**. The parameters of **1-Fe** are similar to those reported for derivatized ferrocenes.[28] δ for **2-Fe** (0.65(4) mm s^{-1}) is slightly more positive than many characterized Fe(I) complexes ($\sim$0.2 to $\sim$0.6 mm s^{-1}),[29] but in good agreement with the low-spin 19 VE [Fe(Cp^{R})(arene)] complexes,[17,30] and in contrast to high-spin **4-Fe** (1.25 mm s^{-1}).[16] We also found excellent agreement between the DFT calculated δ and ΔE_Q parameters and the experimental data (Table 2) for both **1-Fe** and **2-Fe**. Data for **3-Fe** and **4-Fe** is shown for completeness.

To rationalize the structural features of **2-M** with their ground-state electronic structures, we have performed CASSCF/NEVPT2 calculations (see ESI† for details). The *ab initio* ligand field theory (AILFT) derived molecular orbital (MO) diagrams for **1-M**, **2-M**, **3-Fe**, and **4-Fe**, are shown in Fig. 3.[16] The most striking observation is the significant difference in ligand field strength between **2-Fe** and **4-Fe**, which results in a drastic difference between the energetic separation of the d_{z^2} and d_{xz}/d_{yz} orbitals and is responsible for the change in spin-state of **2-Fe** compared to **4-Fe**. This can be rationalized by comparing the L$_{cent}\cdots$Fe distances (L = TMP, avg. 1.713(1) Å; L = Cp^{ttt}, avg. 1.750(3) Å); the closer TMP ligand provides a stronger ligand field than Cp^{ttt}, similar to the situation in high-spin/low-spin manganocenes.[31]

By considering the MO diagram of a 1,1′-diphosphametallocene,[32] which is similar to that of FcH, we can rationalize some of the bond changes.[33] In the MO scheme of D_{5d} symmetric FcH the LUMO is comprised of a doubly degenerate set of antibonding orbitals with ligand e_1'' (for a D_{5h} Cp ring) contributions that mix with the d_{xz}/d_{yz} (e_{1g}) orbitals. The LUMO of 1,1′-diphosphametallocenes is also comprised of metal d_{xz}/d_{yz} orbitals, along with a single ligand HOMO (π_P here, Fig. S36, ESI†) that approximates the Cp e_1'' MOs by having a single nodal plane perpendicular to the ring plane, but has significant contribution from the P-atom. The SOMO of **2-Fe** is principally d_{xz} in character, and is anti-bonding with respect to π_P which explains the increased Fe–P and TMP$_{cent}\cdots$Fe distances. Conversely, as the SOMO for **2-Cr** is comprised of the non-bonding d_{z^2} orbital as it is in **1-Cr**, the structural changes on reduction are minimal. The slight shortening of TMP$_{cent}\cdots$Cr from **1-Cr** to **2-Cr** is related to the change in spin state from $S = 1$ to $S = \frac{1}{2}$ which lowers the energy of the $d_{x^2-y^2}$, d_{xy} orbitals, increasing covalency as in [Cr(Cp)$_2$].[34]

Table 2 Mössbauer parameters for **1-Fe** to **4-Fe**

		1-Fe	2-Fe	3-Fe[b]	4-Fe[b]
δ (mm s^{-1})	Exp.:	0.48(3)	0.65(4)	0.66(2)	1.25(2)
	Theory[a]:	0.50	0.66	0.64	1.09
ΔE_Q (mm s^{-1})	Exp.:	2.02(2)	1.28(4)	2.60(2)	1.23(2)
	Theory[a]:	1.91	1.46	2.52	0.65

[a] Calculated with BP86 and Fe (CP(PPP)), C (def2-tzvp), H (def2-svp) basis set combination. This gave the best agreement with previous experimental results for complexes **3-Fe** and **4-Fe**. [b] From ref. 16.

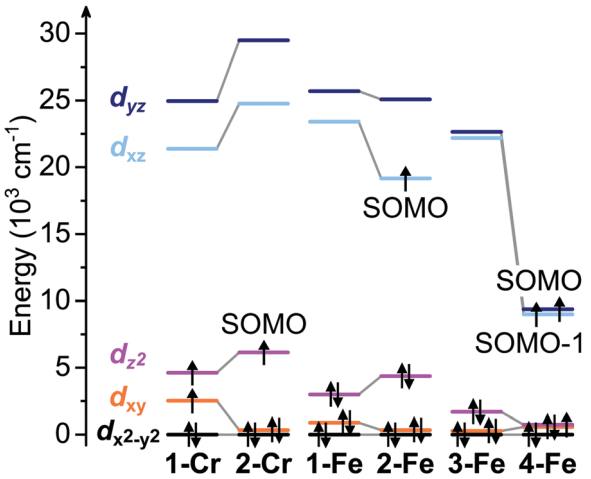

Fig. 3 AILFT orbital energies for the frontier orbitals with principally d-character for **1-M**, **2-M**, **3-Fe** and **4-Fe**.[16] The indicated electronic configuration corresponds to the dominant configuration of the CASSCF + NEVPT2 calculated ground state, and all six complexes feature the same orbital ordering (from low- to high-energy: $d_{x^2-y^2}$, d_{xy}, d_{z^2}, d_{xz}, d_{yz}). The molecular *z*-axis was chosen to align approximately with the vector formed by the metal and ligand ring-centroids. The SOMO orbital(s) of the reduced anionic complexes has been indicated for **2-M** and **4-Fe**.

We suggest that the removal of degeneracy in the ligand HOMO orbitals for TMP *vs.* the equivalent orbitals in Cp lifts the near-degeneracy between the d_{xz}/d_{yz} orbitals (as in **2-Fe** compared to **4-Fe**); and furthermore, the large change in ligand steric profile has drastically changed the separation between d_{z^2} and the d_{xz}/d_{yz} orbitals. These combined effects have stabilized the low-spin state in **2-Fe** and should prove instructive towards chemical control of the spin state in reduced metallocenes and heterometallocenes for the 3d series. For example, by significantly changing the gap between the d_{z^2} and d_{xz}/d_{yz} orbitals in **4-Fe**, a low-spin ferrocenate might be realized.

To summarize, we have demonstrated that octamethyl-1,1′-diphosphametallocenes for Cr and Fe can be reduced to afford crystalline anionic complexes. Comparison of **2-Fe** to authentic formal Fe(I) complexes suggests that it also contains a formal Fe(I). We targeted complexes that might be temperature stable; while **2-Fe** is somewhat thermally unstable, **2-Cr** appears stable indefinitely in the solid-state at room temperature. Both were more amenable to characterization than **4-Fe** which decomposes in the solid-state even at -35 °C.[16] We have found that both anionic species studied here exhibit low spin ($S = \frac{1}{2}$) ground states, in contrast to high-spin ($S = \frac{3}{2}$) **4-Fe**, and that these results are well explained by changes in the ligand frontier orbitals and M–TMP distances. This suggests that synthetic control of the ground spin state of 3d metallocenates is possible and that with judicious planning, it should be possible to target desired high- or low-spin examples of this family.

SMG acknowledges support from a Director's Postdoctoral Fellowship (20180759PRD4), and CAPG was sponsored by a

J. Robert. Oppenheimer Distinguished Postdoctoral Fellowship (20180703PRD1), both through the Los Alamos National Laboratory – Laboratory Directed Research and Development program (LANL-LDRD). CAPG also thanks the UK Engineering and Physical Sciences Research Council (EPSRC) for a Doctoral Prize Fellowship (UoM). An EPSRC grant (EP/K039547/1) provided a single-crystal X-ray diffractometer (UoM). JLK also thanks the LANL-LDRD program. We also acknowledge the University of California and LANL Postdoctoral Entrepreneurial Fellowship and the Feynman Center for Innovation for support of RJB. BWS acknowledges funding provided by the Director, Office of Science, Office of Basic Energy Sciences, Division of Chemical Sciences, Geosciences, and Biosciences, Heavy Element Chemistry Program of the U.S. Department of Energy (DOE). We thank Prof. Michael Shatruk for supervising collection of magnetometry data; and Dr David P. Mills, Dr Fabrizio Ortu, Dr Andrew J. Gaunt and Dr Michael T. Janicke for helpful discussions. We also thank Prof. James M. Boncella for the provision of synthetic work space. A portion of this work was supported by the NSF award CHE-1955754, and performed at the National High Magnetic Field Laboratory under National Science Foundation Cooperative Agreement No. DMR-1644779 with the State of Florida. LANL, an affirmative action/equal opportunity employer, is managed by Triad National Security, LLC, for the NNSA of the U.S. Department of Energy (89233218CNA000001). Raw research data files supporting this publication are available from Figshare at DOI: 10.6084/m9.figshare.13348460. The ESI† contains ORCA input files used in this work.

CAPG lead the project and performed all synthesis, UV-vis-nIR and NMR characterization; and also X-ray diffraction measurements with supervision by BLS. SMG performed EPR and Mössbauer spectroscopies and interpretation and all theoretical work, with supervision by BWS. OU performed SQUID magnetometry measurements and interpretation. RJB sealed samples for analysis and was supervised by JLK. The manuscript was prepared by CAPG with input from all authors.

Conflicts of interest

There are no conflicts to declare.

Notes and references

1 N. J. Long, *Metallocenes: An Introduction to Sandwich Complexes*, Wiley, 1998.
2 A. Togni and R. L. Halterman, *Metallocenes: Synthesis Reactivity Applications*, 1998.
3 (*a*) T. J. Kealy and P. L. Pauson, *Nature*, 1951, **168**, 1039; (*b*) S. A. Miller, J. A. Tebboth and J. F. Tremaine, *J. Chem. Soc.*, 1952, 632; (*c*) J. D. Dunitz, L. E. Orgel and A. Rich, *Acta Crystallogr.*, 1956, **9**, 373.
4 G. Wilkinson, M. Rosenblum, M. C. Whiting and R. B. Woodward, *J. Am. Chem. Soc.*, 1952, **74**, 2125.
5 Š. Toma and R. Šebesta, *Synthesis*, 2015, 1683.
6 R. R. Gagne, C. A. Koval and G. C. Lisensky, *Inorg. Chem.*, 1980, **19**, 2854.
7 (*a*) N. Kuhn, E. M. Horn, R. Boese and N. Augart, *Angew. Chem., Int. Ed. Engl.*, 1988, **27**, 1368; (*b*) O. J. Scherer and T. Brück, *Angew. Chem., Int. Ed. Engl.*, 1987, **26**, 59; (*c*) M. Saito, N. Matsunaga, J. Hamada, S. Furukawa, T. Tada and R. H. Herber, *Chem. Lett.*, 2019, **48**, 163; (*d*) F. Mathey, *Coord. Chem. Rev.*, 1994, **137**, 1.
8 M. Walczak, K. Walczak, R. Mink, M. D. Rausch and G. Stucky, *J. Am. Chem. Soc.*, 1978, **100**, 6382.
9 W. Erb and F. Mongin, *Synthesis*, 2019, 146.
10 B. Deschamps, J. Fischer, F. Mathey and A. Mitschler, *Inorg. Chem.*, 1981, **20**, 3252.
11 B. Deschamps, J. Fischer, F. Mathey, A. Mitschler and L. Ricard, *Organometallics*, 1982, **1**, 312.
12 M. Malischewski, M. Adelhardt, J. Sutter, K. Meyer and K. Seppelt, *Science*, 2016, **353**, 678.
13 (*a*) A. J. Bard, E. Garcia, S. Kukharenko and V. V. Strelets, *Inorg. Chem.*, 1993, **32**, 3528; (*b*) Y. Mugnier, C. Moise, J. Tirouflet and E. Laviron, *J. Organomet. Chem.*, 1980, **186**, C49; (*c*) W. E. Geiger, *J. Am. Chem. Soc.*, 1974, **96**, 2632; (*d*) J. D. L. Holloway, W. L. Bowden and W. E. Geiger, *J. Am. Chem. Soc.*, 1977, **99**, 7089; (*e*) N. Ito, T. Saji and S. Aoyagui, *J. Organomet. Chem.*, 1983, **247**, 301.
14 (*a*) M. Malischewski and K. Seppelt, *Dalton Trans.*, 2019, **48**, 17078; (*b*) J. L. Robbins, N. M. Edelstein, S. R. Cooper and J. C. Smart, *J. Am. Chem. Soc.*, 1979, **101**, 3853; (*c*) J. C. Smart and J. L. Robbins, *J. Am. Chem. Soc.*, 1978, **100**, 3936.
15 F. Hung-Low and C. A. Bradley, *Inorg. Chem.*, 2013, **52**, 2446.
16 C. A. P. Goodwin, M. Giansiracusa, S. M. Greer, H. M. Nicholas, P. Evans, M. Vonci, S. Hill, N. F. Chilton and D. P. Mills, *Nat. Chem.*, 2020, DOI: 10.1038/s41557-020-00595-w.
17 (*a*) D. Astruc, *Tetrahedron*, 1983, **39**, 4027; (*b*) M. Rajasekharan, S. Giezynski, J. Ammeter, N. Oswald, J. Hamon, D. Astruc and P. Michaud, *J. Am. Chem. Soc.*, 1982, **104**, 2400.
18 D. Baudry and M. Ephritikhine, *J. Organomet. Chem.*, 1980, **195**, 213.
19 B. M. Gardner, J. McMaster, W. Lewis and S. T. Liddle, *Chem. Commun.*, 2009, 2851.
20 (*a*) R. Loschen, C. Loschen, W. Frank and C. Ganter, *Eur. J. Inorg. Chem.*, 2007, 553; (*b*) F. Mathey, *J. Organomet. Chem.*, 2002, **646**, 15; (*c*) M. Ogasawara, T. Nagano, K. Yoshida and T. Hayashi, *Organometallics*, 2002, **21**, 3062; (*d*) M. Ogasawara, M. Shintani, S. Watanabe, T. Sakamoto, K. Nakajima and T. Takahashi, *Organometallics*, 2011, **30**, 1487.
21 (*a*) Y. Cabon, D. Carmichael and L. Ricard, *Chem. Commun.*, 2011, **47**, 11486; (*b*) P. Lemoine, M. Gross, P. Braunstein, F. Mathey, B. Deschamps and J. H. Nelson, *Organometallics*, 1984, **3**, 1303; (*c*) N. G. Connelly and W. E. Geiger, *Chem. Rev.*, 1996, **96**, 877.
22 R. Feher, F. H. Köhler, F. Nief, L. Ricard and S. Rossmayer, *Organometallics*, 1997, **16**, 4606.
23 (*a*) A. J. Ashe III, S. Al-Ahmad, S. Pilotek, D. B. Puranik, C. Elschenbroich and A. Behrendt, *Organometallics*, 1995, **14**, 2689; (*b*) F. Nief, F. Mathey, L. Ricard and F. Robert, *Organometallics*, 1988, **7**, 921.
24 **1-Cr** was reported *vs.* the $[Co(Cp)_2]^{+/0}$ couple, and corrected to values *vs.* $FcH^{+/0}$.
25 W. J. Evans, *Organometallics*, 2016, **35**, 3088.
26 G. De Lauzon, B. Deschamps, J. Fischer, F. Mathey and A. Mitschler, *J. Am. Chem. Soc.*, 1980, **102**, 994.
27 (*a*) N. Augart, R. Boese and G. Schmid, *Z. Anorg. Allg. Chem.*, 1991, **595**, 27; (*b*) W. E. Broderick, J. A. Thompson, E. P. Day and B. M. Hoffman, *Science*, 1990, **249**, 401; (*c*) D. P. Freyberg, J. L. Robbins, K. N. Raymond and J. C. Smart, *J. Am. Chem. Soc.*, 1979, **101**, 892.
28 (*a*) R. M. G. Roberts, J. Silver and B. Yamin, *J. Organomet. Chem.*, 1984, **270**, 221; (*b*) R. A. Stukan, S. P. Gubin, A. N. Nesmeyanov, V. I. Gol'danskii and E. F. Makarov, *Theor. Exp. Chem.*, 1966, **2**, 581; (*c*) G. K. Wertheim and R. H. Herber, *J. Chem. Phys.*, 1963, **38**, 2106.
29 J. P. Mariot, P. Michaud, S. Lauer, D. Astruc, A. X. Trautwein and F. Varret, *J. Phys.*, 1983, **44**, 1377.
30 P. Gütlich, E. Bill and A. X. Trautwein, *Mössbauer Spectroscopy and Transition Metal Chemistry*, 2011.
31 M. D. Walter, C. D. Sofield, C. H. Booth and R. A. Andersen, *Organometallics*, 2009, **28**, 2005.
32 N. M. Kostic and R. F. Fenske, *Organometallics*, 1983, **2**, 1008.
33 A. Haaland, *Acc. Chem. Res.*, 1979, **12**, 415.
34 M. Swart, *Inorg. Chim. Acta*, 2007, **360**, 179.

